NIH Public Access
Author Manuscript
*Nucl Med Commun*. Author manuscript; available in PMC 2013 April 1.

Published in final edited form as:
*Nucl Med Commun*. 2012 April ; 33(4): 349–361. doi:10.1097/MNM.0b013e32834ec8a5.

# Review of Functional/ Anatomic Imaging in Oncology

**Stephanie N. Histed**, **Maria L. Lindenberg**, **Esther Mena**, **Baris Turkbey**, **Peter L. Choyke**, and **Karen A. Kurdziel**
Molecular Imaging Program, National Cancer Institute, National Institutes of Health, Bethesda, MD 20892, USA

## Abstract

Patient management in oncology increasingly relies upon imaging for diagnosis, response assessment, and follow-up. The clinical availability of combined functional-anatomic imaging modalities, which integrate the benefits of visualizing tumor biology with those of high-resolution structural imaging, revolutionized clinical management of oncologic patients.[1–6] Conventional high resolution anatomic imaging modalities such as computed tomography (CT) and magnetic resonance imaging (MRI) excel at providing details regarding lesion location, size, morphology, and structural changes to adjacent tissues; however, these modalities provide little insight into tumor physiology. With the increasing focus on molecularly targeted therapies, imaging radiolabeled compounds with positron emission tomography (PET) and single photon emission tomography (SPECT) are often used to provide insight into a tumor's biologic functions and its surrounding microenvironment. Despite their high sensitivity and specificity, PET and SPECT alone are substantially limited by low spatial resolution and inability to provide anatomic detail. Integrating SPECT or PET with a modality capable of providing these (i.e. CT or MR) maximizes their separate strengths and provides anatomic localization of physiologic processes with detailed visualization of a tumor's structure. The availability of multi-modality (hybrid) imaging with PET/CT, SPECT/CT and PET/MR improves our ability to characterize lesions and to affect treatment decisions and patient management. We have just begun to exploit the truly synergistic capabilities of multi-modality imaging. Continued advances in instrumentation and imaging agent development will improve our ability to noninvasively characterize disease processes. This review will discuss the evolution of hybrid imaging technology and provide examples of its current and potential future clinical uses.

### Keywords

Multimodality imaging; PET/CT; SPECT/CT; MR/PET

## Multimodality imaging: the best of both worlds

While taken for granted in current medical practice, advanced imaging is a relatively recent adjunct to medical and surgical therapies. Plain film x-ray and planar gamma scintigraphy have been routinely available only in the last century, and volumetric imaging modalities (PET, SPECT, CT, MR) became available in the 1970's. Each modality has its own strengths and limitations; in general, these technologies can be separated into anatomic and functional

**Corresponding Author**: Karen A Kurdziel, MD Molecular Imaging Program National Cancer Institute 10 Center Dr. Blg 10/Rm B3B403 Bethesda, MD 20892-1088 301-443-0622 (Phone) 301-480-1434 (Fax) Karen.kurdziel@nih.gov.

**Publisher's Disclaimer:** This is a PDF file of an unedited manuscript that has been accepted for publication. As a service to our customers we are providing this early version of the manuscript. The manuscript will undergo copyediting, typesetting, and review of the resulting proof before it is published in its final citable form. Please note that during the production process errors may be discovered which could affect the content, and all legal disclaimers that apply to the journal pertain.

NIH-PA Author Manuscript
NIH-PA Author Manuscript
NIH-PA Author Manuscript

NIH-PA Author Manuscript

NIH-PA Author Manuscript

NIH-PA Author Manuscript

imaging. Anatomic imaging technologies (CT and MR) provide unparalleled structural detail, while functional modalities (PET and SPECT) provide insight into biologic behaviors. [2, 7–8]

CT was developed by Hounsfield et al in 1967, driven in part by the improvement in computer processing power along with volumetric x-ray imaging. Using available computing technology, CT generated high resolution three dimensional reconstructions of patient anatomy using multi-plane x-ray imaging and mathematical computer image reconstruction algorithms. Non-specific iodinated contrast agents are routinely used to visualize blood flow and washout, often delineating areas of abnormal enhancement and uptake which can be used as a surrogate for neoplasm or infection/inflammation.[9–11] Improvements in camera technology such as helical and multi-detector CT (MDCT) yielded even higher spatial resolution with shorter scan times (albeit with higher radiation doses). [12–13] Improvements in software enables volumetric reconstructions and surface rendering of specific organs extending the utility of the volumetric data acquired, as exemplified by CT imaging of the gastrointestinal tract.[14]

Despite the exquisite anatomic details CT provides, it imparts little to no information regarding functional or metabolic activity of tissues. Malignant potential is construed from lesion size, and distortions and displacements of normal tissue. As a result, benign and malignant lesions can overlap in appearance.[11] Early metastatic lymph nodes are often too small to be accurately characterized by CT, resulting in frequent false negative results. Post-surgical changes can distort normal anatomy and may change the structure and morphology of the anatomy sufficiently to mask remaining tumor; these findings on CT can incorrectly suggest areas of abnormal growth or disguise areas of true malignant disease.[8]

Functional information from the biodistribution of radiolabeled drugs or other ligands can be obtained with nuclear imaging; however it characteristically results in noisy images that are low in spatial resolution and comparison with anatomic images is often necessary to interpret the results. Only a small portion of the emitted photons are used to construct the image because most of the photons are never detected. The emitted photons must first traverse heavy lead parallel collimators which only allow photons emitted perpendicular to the camera face to interact with the imaging crystal. Additionally, only photons within a specified energy range, characteristic of the isotope used, are accepted for final image construction to decrease photons scattered from other collimators or through tissues. Clinically useful isotopes emit at least one gamma ray (typically ~59 to 364KeV) that can be “stopped” and detected by the gamma camera's crystal. The development of single photon emission tomography (SPECT), in which planar gamma images are obtained in multiple planes/projections, came on the heels of the development of X-ray CT. The SPECT images are reconstructed to produce a volumetric image with spatial resolution of ~7.5–10 mm.

Another technology used for radiotracer imaging is positron emission tomography (PET). Radionuclides that decay with positron emission, such as Fluorine-18, Carbon-11, Iodine-124 and Oxygen-15, can be imaged with a PET scanner, which provides higher spatial resolution (2–5mm for clinical scanners).[15] The emitted positron quickly encounters an electron, resulting in an annihilation reaction in which two photons each with energy of approximately 511 keV are produced with trajectories approximately 180 degrees opposite to each other. While limited-quality imaging of positrons can be performed using SPECT with ultra-high energy collimators, the PET camera was specifically developed to take advantage of the physical characteristics of positron emitters. By only accepting “coincident” photons, i.e. those that hit opposite sides of a ring detector within nanoseconds of each other, and also are approximately 180 degrees apart, heavy collimation is no longer needed to obtain for high resolution images; thus greatly increasing sensitivity. The added

NIH-PA Author Manuscript

NIH-PA Author Manuscript

NIH-PA Author Manuscript

ability to correct for soft tissue photon attenuation effects, by mathematically integrating a sequentially acquired transmission image, allows for absolute quantification of the radioactivity within a given region of interest. If the specific activity of the radiotracer is known (mCi/ug) then the concentration of the administered compound delivered to the tissue can be determined. [2, 4, 8, 16–17]

Despite the higher resolution of PET images compared with gamma scintigraphy, and its ability to measure isotopes with high sensitivity and specificity down to 100 picomolar concentrations,[18] these images still lack spatial resolution compared with imaging modalities such as CT and MRI.

The benefits of hybrid (simultaneous or sequential multi-modality imaging on a single instrument) have been discussed in the medical literature as early as the 1960s[7]. Attempts to visually co-localize lesions to identify the anatomic location of radiotracer uptake proved cumbersome and less than ideal as discrepancies in patient position, patient motion, and imprecise alignment were encountered as the patient moved between two different machines.[2, 4, 6–7, 19]

Software fusion algorithms were developed to permit registration and overlay display from independently acquired images with increasing accuracy and precision.[20] Such algorithms proved to be most useful and accurate in cerebral imaging as the brain is clearly defined and rigidly fixed within the skull, which is used as the primary registration object. This method was less successful in whole body imaging where landmarks are sparse, surface markers are of limited value because of intrinsic motion of visceral organs, the requirement for non-rigid registration capabilities exists and, often, the mutual image information on which to base a registration is lacking.[21–25] As a result of these limitations, the hardware fusion option of combining anatomic and functional imaging into the same gantry in the form of PET/CT was proposed and implemented. An additional benefit of the in-line CT is that it can be used for attenuation correction as well as anatomic localization, with a CT transmission scan acquisition time of <1min compared with ~12 minutes for a conventional transmission scan, which rotates a radioactive source around the patient.

With the increasing clinical utilization of F-18 fluorodeoxyglucose (FDG) PET in oncology, came the demand for more accurate anatomic localization of foci of increased radiotracer uptake. Townsend, Nutt, Beyer and coworkers are credited with developing the first hybrid PET and CT scanning equipment in the late 1990s. After receiving an NCI grant in 1995, the first prototype was built and put into clinical use for oncologic imaging at the University of Pittsburgh Medical Center in 1998, where it operated until 2001. On this instrument, 300 patients with a range of oncologic diagnoses were imaged.[26] Results from this prototype helped to stimulate further development and construction of combined PET/CT scanners. [26–28] Most commercial whole body PET scanners now come with an integrated CT scanner.

Though PET/CT is currently more widely used than SPECT/CT, some of the earliest attempts to obtain functional and anatomic information from a single device were obtained with SPECT technology. In 1988, Butler et al used SPECT, and a separate Gadolinium-153 source to obtain emission and transmission data on a 99mTc-macroagreggated albumin perfusion study to verify proper positioning of an arterial catheter during chemotherapy administration. Acquiring both sets of information improved spatial localization as well as attenuation correction and demonstrated the promising clinical applications of anatomically mapping scintigraphic activity in one session.[29]

Hasegawa and colleagues were pioneers in combining SPECT and CT into a single modality.[30] By 1999, the first commercially available SPECT/CT camera was developed,

NIH-PA Author Manuscript

NIH-PA Author Manuscript

NIH-PA Author Manuscript

incorporating a low energy transmission CT for localization, and SPECT functional images in one system.

Despite more limited clinical use of SPECT/CT, due in part to longer scan times and lack of reimbursement, compared with PET/CT, evidence of improvement in patient care and management has been described. Recent studies have demonstrated increased accuracy and reporter confidence with SPECT/CT compared with SPECT alone.[31–32] In these studies, improvements in lesion localization occurred in greater than 40% of patients. The use of both traditional and novel PET and SPECT imaging agents has allowed for visualization of biologic processes ranging from glucose metabolism to bone remodeling and angiogenesis. Research on radiotracers has brought into focus the necessity of understanding the interplay between physical characteristics of the radiolabeled drug and the target being imaged. Currently, molecular imaging research is focused on developing new radiotracers for both SPECT/CT and PET/CT technology, with an eye toward the of clinical utilization PET/MR and SPECT/ MR, which can provide metabolic and anatomic information with less ionizing radiation. Table 1 contains a listing of selected PET and SPECT imaging agents discussed in this review.

## Clinical Examples

### Bone imaging with PET/SPECT/CT

**$^{99m}$Tc-Methyl-diphosphonate (MDP)—**Bone scans commonly utilize planar gamma camera technology. They consist of whole body bone scintigraphy with $^{99m}$Tc labeled methylene diphosphonate ($^{99m}$Tc-MDP, $t_{1/2}$ = 6h) for detection of bony metastases. (Figure 1a) $^{99m}$Tc hydroxymethylene diphosphonate ($^{99mTc}$-HDP) is very similar and often is used for the same purpose. $^{99m}$Tc is the most frequently used nuclear medicine isotope due to its desirable imaging properties and can be generated on-site from its parent atom, $^{99}$Mo ($t_{1/2}$ = 67h). It should be noted that there have been several worldwide shortages of $^{99}$Mo, which is generated in a limited number of medical nuclear reactors worldwide. In the 1970s $^{99m}$Tc was successfully chelated to polyphosphates and pyrophosphate for skeletal imaging, and quickly became one of the most frequently performed nuclear medicine procedures.[33–35] The pyrophosphate compounds were soon recognized to be inferior to the diphosphonates as imaging compounds, and subsequently $^{99m}$Tc –MDP, demonstrating the best clearance qualities of these diphosphonates, became the gold standard for bone scintigraphy. [33–35]

Whole body bone scintigraphy with$^{99m}$Tc compounds (BS) is routinely used in patients with a known primary cancer, as skeletal involvement occurs in 30–70% of all patients with cancer. BS has high sensitivity in detecting metastatic foci even in lesions with as little as a 5–10% bone loss. In contrast, plain radiography often requires more than a 50% destruction of bone for a lesion to be detected.[36] The sensitivity of BS is 62%–100%, depending on the nature of the lesion, with osteolytic lesions representing the lower end and osteoblastic lesions representing the higher end of the sensitivity range.[37] Planar imaging is efficient, but SPECT, especially with CT, has been found to more precisely localize bone lesions.[38] This is particularly true in the spine, where vertebral body uptake can be indicative of malignancy or degenerative bone disease.[38] SPECT can overcome some of the difficulties found with planar scans and also can help to differentiate overlapping structures; however, anatomic modalities such as CT are still often needed to confidently localize skeletal areas of abnormal uptake.[39]

SPECT/CT image fusion demonstrated improvement over planar BS and SPECT alone in both sensitivity and specificity. Additionally, diagnostic accuracy and certainty increased significantly with hybrid imaging. A decrease in equivocal lesions was found by Zhao et al[40] and Helyar et al[41]. In a study by Strobel et al, diagnosis was made in 100% of cases

NIH-PA Author Manuscript

NIH-PA Author Manuscript

NIH-PA Author Manuscript

on SPECT/CT fusion compared to 86% and 64% when using SPECT or CT alone, respectively.[42]

**Sodium Fluoride ($^{18}$F-NaF) Bone Scanning—**Advances in PET/CT have not only spurred research into novel, more specific radiotracers, but have also stimulated renewed interest in those which had fallen out of use because of challenges in technology. A good example of this is sodium fluoride, $^{18}$F-NaF, identified nearly 50 years ago as a radiotracer for bone imaging.[43] This agent shows high and rapid bone uptake and clearance from other body compartments and yielding high quality, low background images within one hour after injection..[33, 44] $^{18}$F-NaF which is minimally bound by proteins in the serum, has a highfirst pass extraction rate at physiologic blood flow, and demonstrates preferential uptake in areas of actively mineralizing bone.[45]

Though available for patient use in the 1970s after approval by the FDA, $^{18}$F-NaF did not gain clinical momentum since PET scanners were not yet prevalent and imaging this compound on SPECT cameras proved suboptimal. Also, in the 1970s, $^{99m}$-Tc bone agents became readily available as they could be compounded using “kits” in on-site radiopharmacies. In contrast, $^{18}$F-NaF is cyclotron generated with a 110 minute half-life and, at the time,, its distribution was not economically viable. Recent shortages of $^{99m}$Tc, advances in PET scanning equipment and the commercial availability of $^{18}$F have driven a renewed interest in $^{18}$F-NaF as a feasible bone imaging agent.[44] In 1984, the FDA listed $^{18}$F-NaF as a discontinued drug but made it available under “Investigational New Drug” (IND) status. More recently, the NCI has filed a New Drug Application (NDA) which was approved by the FDA, making this agent available for use in patients for clinical management.[46]

Effective February 26, 2010 the Center for Medicare and Medicaid Services (CMS) announced that $^{18}$F NaF PET imaging used to “inform initial treatment strategy (PI) or subsequent treatment strategy( PS) for suspected or biopsy proven bone metastasis” are covered, when performed in the context of a clinical study. [47]

Because of the increased resolution, sensitivity and specificity of PET/CT compared with that of SPECT/CT, abnormal areas of $^{18}$F-NaF uptake are more readily apparent than with $^{99m}$Tc-MDP. In some groups of patients, such as those with metastatic prostate cancer, it is expected that metastatic disease can be detected much earlier with $^{18}$F-NaF PET than with conventional bone scans. However, similar to $^{99m}$Tc-MDP, $^{18}$F-NaF uptake alone will not differentiate between benign and malignant disease; thus, the CT component of the study is critical to distinguish the cause of increased uptake. [46]

Recent studies have compared $^{99m}$Tc bone agents with $^{18}$F-NaF in patients with both benign and malignant bone lesions; a review of these by Grant et al. in 2007 found $^{18}$F-NaF PET imaging is more accurate than planar imaging or SPECT for lesion characterization and localization in both malignant and benign lesions. (Figure 1) Additionally, $^{18}$F-NaF PET/CT reduces length of study scan time, and improves clinic workflow and convenience to the patient. More recently, studies have compared $^{18}$F-NaF PET/CT scanning for bone disease with $^{99m}$Tc-MDP in patients with hepatocellular carcinoma suspected of having bony metastases. The study found that the $^{18}$F-NaF had better sensitivity and specificity for detecting bony lesions, specifically primarily osteolytic lesions. The authors also found an increase in accuracy by PET/CT with $^{18}$F-NaF compared with $^{99m}$Tc-MDP (95.7% vs. 75.4%, respectively, P=0.0001) and a significant correlation between prognosis and bony lesions found on $^{18}$F scan; such a relationship was not found with $^{99m}$Tc-MDP.[48] Similar results were found in patients with non-small cell lung cancer.[49] This increased accuracy, along with the current availability of PET/CT technology in a range of clinical settings and

NIH-PA Author Manuscript

NIH-PA Author Manuscript

NIH-PA Author Manuscript

the relative ease at producing $^{18}$F, indicate this technology will become increasingly incorporated into routine clinical use.[33]

## Tumor Imaging

**$^{18}$F-Fluorodeoxyglucose ($^{18}$F-FDG)—**By far the most frequently used PET agent for oncology, the glucose analog formally known as 2-[fluorine-18] fluoro-2-deoxy-D-glucose or more informally as $^{18}$F-FDG [50] has been extensively dicussed elsewhere, therefore, only a cursory discussion will be made here. $^{18}$F-FDG was first described as a potential tumor biomarker in 1980, after several years use as a brain imaging agent.[51] $^{18}$F-FDG accumulates in tissues with high metabolic activity as a result of trapping within the cell. Although $^{18}$F-FDG is transported into the cell as if it were glucose via the GLUT 1 transporter, unlike glucose, it is blocked from further phosphorylation. Normally, glucose is phosphorylated to glucose-6-phosphate by hexokinase, an enzyme up-regulated in malignant cells [16, 51–52]. Therefore, the elevation of hexokinase drives increased uptake of both glucose and $^{18}$F-FDG by tumor cells. PET imaging with $^{18}$F-FDG allows the non-invasive detection of abnormal metabolic activity in malignancies; a feat that is not achievable with conventional anatomic scanning.

$^{18}$F-FDG PET has had extraordinary clinical reach, with a contribution unmatched by any other functional imaging modality to date.[53] It has been used in the diagnosis, treatment planning, monitoring of treatment response, and follow-up for recurrence after treatment in many oncologic disease processes.[1–3, 5–6, 8–9, 16] A recent review of the literature regarding the use of $^{18}$F-FDG PET found its use most clinically effective in staging non-small cell lung carcinoma, restaging Hodgkin's lymphoma, detecting solitary pulmonary nodules, and staging or restaging colorectal carcinoma.[54] However, since its widespread introduction, it has found utility in virtually every tumor type for at least one application.

Combining $^{18}$F-FDG PET with CT has led to an improvement of accuracy averaging about 10–15% compared with PET alone.[44] Such benefits have been described in patients with head and neck, thyroid, breast, lung, and GI tract carcinomas, tumors of unknown primary origin, melanomas and also lymphomas.[5, 44]

Despite the improved sensitivity and specificity of $^{18}$F-FDG PET localization, a number of limitations have emerged. $^{18}$F-FDG is taken up at a higher rate by malignant tissue; however, it is not specific for tumor cells. Indeed, other processes which result in increased metabolic activity, such as inflammatory and infectious states are avid for $^{18}$F-FDG, thus leading to false positives (Figure 2). Normal tissues can also take up or accumulate $^{18}$F-FDG including bowel, bladder, muscle, and brown fat, all of which can demonstrate higher-than-background activity.[11] Furthermore, $^{18}$F-FDG has low sensitivity for tumors of low grade, low glucose uptake and size <1cm.[50] Some malignant tumors do not readily metabolize $^{18}$F-FDG, including bronchioloaveolar carcinoma,[55] NETs, renal cell carcinomas and localized prostate cancer.[56] Additionally, in organs with high $^{18}$F-FDG excretion such as the bladder and kidneys, significant background activity limits evaluation of lesions in those tissues. As a result, other PET agents have been evaluated for use in oncology.

## Somatostatin receptor imaging

Neuroendocrine tumors (NET) are a varied group of neoplastic lesions which arise from neuroendocrine cells of the lung, thymus, pancreas, GI tract, adrenals, and skin, and thus, are an extremely heterogeneous group of cancers.[57] They do share common characteristics, namely their origin from cells with a neuroendocrine function that take up and decarboxylate amines. The term APUD (amine precursor uptake and decarboxylation) cell was coined for

NIH-PA Author Manuscript

NIH-PA Author Manuscript

NIH-PA Author Manuscript

these neuroendocrine cells by Pearse in the 1960s.[58–61] More specifically, they originate from embryonic neural crest cells, and their varied location within the body is attributable to anatomic structures arising from the embryonic foregut, midgut, or hindgut. A feature common to some, but not all, NETs is the expression of somatostatin receptors (SSTRs), particularly SSTR-2, SSTR-5 and to a lesser extent SSTR-3. This characteristic has been exploited for their diagnosis and treatment.[62–63]

Because they can be found in many locations throughout the body and often present with clinical symptoms at a relatively small size, NETs are difficult to locate using anatomical imaging techniques. Functional imaging, using a variety of SPECT compounds, has played a large role in the diagnosis and characterization of these tumors. By primarily targeting somatostatin receptors commonly expressed on these tumors,[57] SPECT agents targeting somatostatin receptors have been developed, including $^{111}$In-diethylenetriamine pentaacetic acid (DTPA)-pentreotide (Octreoscan®), and more recently $^{99m}$Tc-ethylene diamine N,N'-diacetic acid/hydrazinonicotinamide (EDDA/HYNIC)-tyr3-octreotide.[64–65], and $^{68}$Ga-DOTA-Tyr(3)-octreotide or octreotate. Though $^{99m}$Tc is a better SPECT agent than $^{111}$In, and initial results from small studies using $^{99m}$Tc-EDDA/HYNIC-TOC show promising results, $^{111}$In-DTPA-pentreotide is the standard agent in clinical use today.[64]

Practice guidelines for imaging of NETs with $^{111}$In-DTPA-pentreotide have been published by the Society for Nuclear Medicine and European Association for Nuclear Medicine. They describe the use of this agent in NETs including, but not limited to, those tumors of the adrenal medulla, merkel cell of the skin, gastropancreatic system, and pituitary. It has been a helpful imaging tool in other malignancies as well, such as melanomas, small cell lung carcinomas, and carcinoid tumors.[66–67] A dose of 6 mCi of $^{111}$In-DPTA-pentetreotide is suggested, and use of SPECT/CT is highly recommended.[64] (Figure 3)

While not yet FDA approved, small clinical studies have shown $^{68}$Ga- octreotide derivative 4,7,10-tetraazacyclo-dodecane-N,N′,N″,N‴-tetraacetic-acid-D-Phe1-Tyr3-octreotide (DOTA-TOC), a PET radiotracer, to be superior to SPECT imaging agents $^{111}$In-DPTA-pentetreotide [68], and $^{123}$I-metaiodobenzylguanidine (MIBG; a.k.a. iobenguane or Adreview).[69]. $^{68}$Ga is a positron emitter obtained from a $^{68}$Ge/$^{68}$Ga generator (half-life, 270.8 days). Disappointingly, $^{68}$GaDOTA TOC PET/CT, showed no advantage over conventional imaging in monitoring response to peptide related radionuclide therapy (using either $^{90}$Y-DOTA-TOC or $^{177}$Lu-DOTA-octreotate). [70]

**$^{18}$F-FLT—**[$^{18}$F]-3'-fluoro-3'-deoxy-L-thymidine (FLT) is a fluorinated thymidine analog that accumulates in highly proliferating cells.[71–73] Originally, non-radioactive FLT was developed as an anti-viral therapy in HIV infection but proved too toxic. However,it is safe in the microdoses used for clinical imaging.

Thymidine is incorporated into DNA as one of the four basic nucleosides (adenine thymine, cytosine, guanine). Initial studies with $^{11}$C-thymidine demonstrated more rapid declines in uptake after cancer therapy than with $^{18}$F-FDG scans.[74–76] However, the short half-life of $^{11}$C (˜20min) and its rapid metabolism *in vivo* limited its use to research settings; subsequently, labeling the thymidine analog fluoro-L-thymidine (FLT) with $^{18}$-F was undertaken.[71] Once it is transported into a cell, it is phosphorylated via thymidine kinase -1 and becomes trapped intracellularly. While, for the most part, it is not incorporated into DNA, the regulation of thymidine kinase-1 is closely related to cell proliferation status; cells in the G1 to S phases of the cell cycle demonstrate up to 20-fold higher rates of TK-1 activity compared to cells in G0 or the onset of G1.[77] FLT is useful because it reflects cellular proliferation as determined by proliferating cell nuclear antigen (PCNA) and Ki-67

NIH-PA Author Manuscript

NIH-PA Author Manuscript

NIH-PA Author Manuscript

score. A detailed description of the cellular retention of FLT via the purine salvage pathway is reviewed by Salskov et al.[73]

Because of FLT's specificity for cellular replication, its most promising use lies as an imaging agent, to characterize tumors and predict their response to therapy.[78] However, compared with $^{18}$F-FDG, $^{18}$F-FLT has a lower uptake by tumor cells since not all cells are in an active replication stage.[73, 78] $^{18}$F-FLT demonstrates physiologic accumulation in liver and bone marrow in higher amounts than $^{18}$F-FDG. While $^{18}$F-FLT is less sensitive than $^{18}$F-FDG for tumor detection, it can add specificity, as it does not show high uptake in inflammatory tissues, a limitation of $^{18}$F-FDG (FIGURE 4). As the prevailing dogma predicts highly proliferating cells to be more sensitive to the effects of cytotoxic therapies, determining which tumors are highly proliferative prior to therapy may help with the selection of therapy. [77]In some tumors,$^{18}$F-FLT uptake has been shown to decrease even before physical changes in lesion size can be measured, and before a decrease in $^{18}$F-FDG PET is seen.[77] This decrease was found to correlate with decreased malignant cellular proliferation. $^{18}$F-FLT has also been evaluated across a wide range of primary tumors, including lung, breast, brain, colon, esophageal, and head and neck malignancies as well as lymphoma, melanoma, and sarcoma.[73, 78] With the exception of one trial involving patients with rectal cancers, the decrease in $^{18}$F-FLT activity after beginning chemotherapy regimens was predictive of tumor response.[77] As noted recently by Del Vecchio et al, the initial post-therapy FLT scan must be performed early in the regimen in order to reflect the true anti-proliferative effects of the treatment. [77] Due to its limited ability to stage tumors, especially compared with $^{18}$F-FDG PET, $^{18}$F-FLT has been suggested as an important adjunct, but not a stand-alone modality, for oncologic imaging. Further applications of FLT include investigations into the assessment of tumor aggressiveness and patient response to therapy.

## Imaging Tumor Angiogenesis

Tumor cells generate factors to promote neo-vascularization for continued survival and growth. In fact, without angiogenesis, tumors stop growing both *in vitro* and *in vivo* at a diameter of 2–3mm.[79] Thus, angiogenesis has been vigorously investigated in order to understand the mechanisms involved and to exploit them for cancer therapy.

The first commonly used targeted antiangiogenic drug, the monoclonal antibody bevacizumab, which targets the vascular endothelial growth factor (VEGF), was approved in 2004. Since then, additional small molecule inhibitors of angiogenesis have been clinically approved including sorafenib and sunitinib.; these agents are directed against VEGF and platelet-derived growth factor (PDGF) receptors.[18, 80] These agents work in a cytostatic rather than cytotoxic manner[18], and thus, present difficulty when evaluating patient response to therapy using the gold standard of tumor volume change on CT or MRI. Anti-angiogenic therapies will not necessarily result in a marked tumor volume reduction on conventional imaging; therefore, imaging agents targeting the angiogenesis pathway may be valuable in predicting and monitoring patient response to treatment. There are numerous competing technologies for measuring angiogenesis. These include dynamic CT, MRI and microbubble enhanced ultrasound. However, these methods are indirect measures of angiogenesis, measuring parameters such as blood flow and permeability rather than angiogenesis itself.

The ability to label specific molecular angiogenic markers with trace amounts of radionuclides is a very promising molecular imaging method. A variety of targets have been identified for PET imaging of angiogenesis including $\alpha_v\beta_3$ integrin, VEGF and VEGFR ligands, matrix metalloproteases, and hypoxia factors.[77, 81] Integrins are a group of 24 membrane proteins that function as endothelial cell adhesion molecules involved in cellular

NIH-PA Author Manuscript

NIH-PA Author Manuscript

NIH-PA Author Manuscript

attachment and migration to the extracellular matrix.[82–83] Some tumor cells over-express integrins, which appear to have a role in promoting cellular migration and metastases. The integrins are comprised of two non-covalently linked subunits, α and β, and this heterodimeric structure forms a protein expressed at the cell membrane.[77, 81–83] $\alpha_v\beta_3$ integrin is the most extensively studied of the family, and it is up-regulated significantly in tumor vasculature but not in normal endothelium.[84–88] Crystallography structure has identified the amino acid sequence arginine-glycine-aspartic acid (RGD) as the common binding motif to $\alpha_v\beta_3$ integrin. To date, many conjugates with this sequence have been prepared and labeled for optical imaging, MRI, SPECT, and PET. $^{18}$F, $^{64}$Cu, and $^{68}$Ga have all been attached to RGD analogs to bind to $\alpha_v\beta_3$ integrin.[82–83, 89] The first integrin imaging agent used in humans was $^{18}$F-galacto-RGD, which demonstrated good tumor uptake with low tumor to background ratios and rapid clearance from non-tumor tissue.[89–92] Uptake of $^{18}$F-galacto-RGD correlates with microvessel density.[93] Numerous studies have demonstrated the ability of $^{18}$F-galacto-RGD to bind to $\alpha_v\beta_3$ integrin to image tumor vasculature. Little correlation is seen between $^{18}$F-FDG and $^{18}$F-galacto-RGD signal, indicating distinct information is being provided by each tracer.[92] Unfortunately, the synthesis of $^{18}$F-galacto-RGD is complex and is not widely transferrable to the clinical setting. Thus, other radiolabeled compounds targeting the RGD binding pocket are under development. Figure 5 shows a PET/CT image of $^{18}$F-Fluciclatide, a small fluorinated peptide containing the RGD sequence.

$\alpha_v\beta_3$ integrin expression is not limited to tumor endothelial cells [92–93] and has also been identified in wound healing, rheumatoid arthritis, and other inflammatory states.[94] Thus, research into integrins specifically expressed on activated endothelial cells, such as $\alpha_5\beta_1$, has been actively pursued.[93] Additionally, integrin targeted-agents coupled to nanoparticles are being investigated as they do not extravagates from vessels, thereby facilitating imaging of only the vasculature and providing a better measure of the angiogenesis network.[83] These nanoparticle agents are being developed with an eye toward multimodality imaging techniques, as small molecules, such as $^{18}$F-galacto-RGD, are restricted by limited conjugation sites and binding affinity interference; these problems can be overcome by utilizing the large surface area of nanoparticles.[82]

## Future of multimodality imaging

**MR/PET imaging—**When compared with CT, MR provides superior soft-tissue contrast and imposes no ionizing radiation. It can also provide some functional information through use of MR spectroscopy, diffusion imaging and perfusion imaging. For combined functional scanning with PET, however, the software registration problems discussed earlier also apply to registering PET and MR images acquired on separate machines. Additional challenges in registering these two separate modalities arise from a smaller field of view, which provides less data and less mutual information (i.e. bony anatomy) with which to perform the registration, and the non-isometric pixel size of MR data. The best chance of achieving a good software-based registration of PET/MR would result from registering the smaller field of view MR to CT slices from a similar field of view from the PET/CT study, which would then put the MR into the same “imaging space” as the PET. Development of such software based registration is exceedingly difficult when imaging organs without intrinsic contrast on CT (i.e. the prostate). FIGURE 6 depicts a software based registration of a prostate MR to a $^{11}$C-acetate PET/CT. Due in part to anatomic distortion of the prostate by the MR endorectal coil, an issue not present with PET/CT, and the mobility of the prostate within the pelvic cavity, only the initial rigid registration between the MR and a limited field-of view extract of the transmission CT could be automated. The final rotation and translation adjustment had to be performed manually based on visual assessment. Attempts to automatically register the MR directly to the whole body transmission CT or to the $^{11}$C-

NIH-PA Author Manuscript

NIH-PA Author Manuscript

NIH-PA Author Manuscript

acetate PET emission scan directly failed due to lack of mutual information between the studies. It is in such applications, where the high soft tissue contrast of MR is needed to localize the functional activity identified on PET, that a combined PET/MR scanner would have the highest impact.

Numerous technical challenges faced the development of a combined PET/MR as the magnetic field of the MRI made PET scanning with conventional cameras impossible.[95] Moreover, the proximity of the PET instrumentation disturbed the magnetic field homogeneity of the MR interfering with image quality. The magnetic field required numerous PET camera electronic and hardware changes in order to maintain functionality. In an integrated system, where the PET camera resides within the MR camera, the maximum bore size may be reduced and there are substantial increases in scattered and random coincidences due to the presence of MR hardware (RF coils) in the field of view.

While this would not be a problem with a sequential design, in which the patient is scanned on each separate modality “sequentially” using the same imaging bed[96] without re-positioning, any design will reduce the quantitative capability of the PET camera as MR data consists of proton densities and magnetic relaxation times with no information about photon attenuation. [97]

Instead of directly measuring photon attenuation as with CT, the attenuation correction with MRI is obtained using segmentation of air, soft tissue and/or bone and then using pre-calculated density measurements to estimate attenuation; however this inevitably results in non-uniform results throughout the field of view. Work to reduce the quantitative degradation by improving the attenuation correction algorithms is ongoing. {Catana, 2011 #205;Schulz, 2011 #204} The most notable problem with PET/MR devices is their cost, which essentially combines the cost of a full MR with a full PET scanner. Additional drawbacks include increased imaging times of MR compared to CT.[98] Additionally, the inability to image patients with contraindications to MR or of wide girth due to a smaller field of view further limits this modality. Another major challenge is the lack of technologists who are trained in both modalities. However, the advantages are also clear. The ability to simultaneously image by MR and PET will mean better localization of PET signal and reduced overall scanning times for patients who require both an MR and PET.

Marsden and Cherry developed the first simultaneous PET/MR for animals (Shao *et al* 1997), demonstrating the feasibility of the method. This was followed by the development of a dedicated brain clinical PET/MR scanner. More recently, whole body clinical PET/MR systems have been produced. Figure 7 With simultaneous acquisitions of PET and MR data, MR's ability to monitor motion (without ionizing radiation) can be exploited to improve PET. For instance, it may be possible to obtain data regarding the direction and magnitude of patient motion occurring during the PET acquisition {Catana, 2011 #205} (i.e. breathing), to accurately localize counts that would otherwise be blurred across the path of motion.

Despite its current limitations and expense, the development of combined PET/MR scanners will continue as such technology opens new vistas for molecular imaging.

## Summary

PET/CT and SPECT/CT technologies have had a far reaching influence on diagnosis, management, therapy monitoring, and prognosis in oncologic disease; they provide more personalized care to patients, improve treatment decisions and help to decrease the cost of medical care in many situations. It is expected that PET/MR will continue this trend.

NIH-PA Author Manuscript

NIH-PA Author Manuscript

NIH-PA Author Manuscript

In recent years, knowledge about cellular processes resulting in cancer has dramatically expanded. New targets for therapy, clinical monitoring and patient management have emerged as a consequence. At the same time, great strides are being made in developing highly specific imaging probes. This is stimulating the development of new imaging technology, including hybrid scanning technology. These new targeted probes may be used in concert with new drugs to accelerate the approval process and select patients for the most appropriate therapy. The ability to combine the sensitivity and specificity of PET with the anatomic resolution of CT has proven invaluable, with documented gains in accuracy. In the future the fusion of any two or more modalities should be possible including SPECT, PET, MR, or even ultrasound. Thus, the future of hybrid imaging remains bright and will hopefully prove useful in the management of patients with cancer.

## Acknowledgments

The authors would like to thank Corina Millo, MD of the PET department, NIH Clinical Center, Bethesda, MD.

## References

1. Weber WA, Avril N, Schwaiger M. Relevance of positron emission tomography (PET) in oncology. Strahlenther Onkol. 1999; 175(8):356–73. [PubMed: 10481766]
2. Maurer AH. Combined imaging modalities: PET/CT and SPECT/CT. Health Phys. 2008; 95(5): 571–6. [PubMed: 18849691]
3. Mariani G, et al. A review on the clinical uses of SPECT/CT. Eur J Nucl Med Mol Imaging. 37(10): 1959–85. [PubMed: 20182712]
4. Townsend DW. Combined positron emission tomography-computed tomography: the historical perspective. Semin Ultrasound CT MR. 2008; 29(4):232–5. [PubMed: 18795489]
5. Bockisch A, et al. Hybrid imaging by SPECT/CT and PET/CT: proven outcomes in cancer imaging. Semin Nucl Med. 2009; 39(4):276–89. [PubMed: 19497404]
6. Townsend DW. Positron emission tomography/computed tomography. Semin Nucl Med. 2008; 38(3):152–66. [PubMed: 18396176]
7. Townsend DW. Multimodality imaging of structure and function. Phys Med Biol. 2008; 53(4):R1–R39. [PubMed: 18263942]
8. Delbeke D, et al. Hybrid imaging (SPECT/CT and PET/CT): improving therapeutic decisions. Semin Nucl Med. 2009; 39(5):308–40. [PubMed: 19646557]
9. Saif MW, et al. 18F-FDG positron emission tomography CT (FDG PET-CT) in the management of pancreatic cancer: initial experience in 12 patients. J Gastrointestin Liver Dis. 2008; 17(2):173–8. [PubMed: 18568138]
10. Gorospe L, et al. Whole-body PET/CT: spectrum of physiological variants, artifacts and interpretative pitfalls in cancer patients. Nucl Med Commun. 2005; 26(8):671–87. [PubMed: 16000985]
11. Wechalekar K, Sharma B, Cook G. PET/CT in oncology--a major advance. Clin Radiol. 2005; 60(11):1143–55. [PubMed: 16223611]
12. Kohl G. The evolution and state-of-the-art principles of multislice computed tomography. Proc Am Thorac Soc. 2005; 2(6):470–6. 499–500. [PubMed: 16352750]
13. O'Connor MK, Kemp BJ. Single-photon emission computed tomography/computed tomography: basic instrumentation and innovations. Semin Nucl Med. 2006; 36(4):258–66. [PubMed: 16950143]
14. Ba-Ssalamah A, et al. Dedicated multi-detector CT of the esophagus: spectrum of diseases. Abdominal imaging. 2009; 34(1):3–18. [PubMed: 17653787]
15. Bray M, et al. Radiolabeled antiviral drugs and antibodies as virus-specific imaging probes. Antiviral Res. 2010; 88(2):129–42. [PubMed: 20709111]
16. Kapoor V, McCook BM, Torok FS. An introduction to PET-CT imaging. Radiographics. 2004; 24(2):523–43. [PubMed: 15026598]

NIH-PA Author Manuscript

NIH-PA Author Manuscript

NIH-PA Author Manuscript


17. Townsend DW, et al. PET/CT today and tomorrow. J Nucl Med. 2004; 45(Suppl 1):4S–14S. [PubMed: 14736831]
18. Niu G, Chen X. PET Imaging of Angiogenesis. PET Clin. 2009; 4(1):17–38. [PubMed: 20046926]
19. Beyer T, Townsend DW. Putting 'clear' into nuclear medicine: a decade of PET/CT development. Eur J Nucl Med Mol Imaging. 2006; 33(8):857–61. [PubMed: 16794821]
20. Levin DN, et al. Retrospective geometric correlation of MR, CT, and PET images. Radiology. 1988; 169(3):817–23. [PubMed: 3263666]
21. Bergstrom M, et al. Head fixation device for reproducible position alignment in transmission CT and positron emission tomography. J Comput Assist Tomogr. 1981; 5(1):136–41. [PubMed: 6972391]
22. Goerres GW, et al. PET-CT image co-registration in the thorax: influence of respiration. Eur J Nucl Med Mol Imaging. 2002; 29(3):351–60. [PubMed: 12002710]
23. Hutton BF, Braun M. Software for image registration: algorithms, accuracy, efficacy. Semin Nucl Med. 2003; 33(3):180–92. [PubMed: 12931320]
24. Reinartz P, et al. Side-by-side reading of PET and CT scans in oncology: which patients might profit from integrated PET/CT? Eur J Nucl Med Mol Imaging. 2004; 31(11):1456–61. [PubMed: 15248033]
25. Slomka PJ. Software approach to merging molecular with anatomic information. J Nucl Med. 2004; 45(Suppl 1):36S–45S. [PubMed: 14736834]
26. Charron M, et al. Image analysis in patients with cancer studied with a combined PET and CT scanner. Clin Nucl Med. 2000; 25(11):905–10. [PubMed: 11079589]
27. Beyer T, et al. A combined PET/CT scanner for clinical oncology. J Nucl Med. 2000; 41(8):1369–79. [PubMed: 10945530]
28. Townsend DW, Beyer T. A combined PET/CT scanner: the path to true image fusion. Br J Radiol. 2002; 75(Spec No):S24–30. [PubMed: 12519732]
29. Butler SP, et al. SPECT evaluation of arterial perfusion in regional chemotherapy. J Nucl Med. 1988; 29(5):593–8. [PubMed: 3259622]
30. Lang TF, et al. Description of a prototype emission-transmission computed tomography imaging system. J Nucl Med. 1992; 33(10):1881–7. [PubMed: 1403162]
31. Roach PJ, et al. SPECT/CT imaging using a spiral CT scanner for anatomical localization: Impact on diagnostic accuracy and reporter confidence in clinical practice. Nucl Med Commun. 2006; 27(12):977–87. [PubMed: 17088684]
32. Schillaci O, et al. Is SPECT/CT with a hybrid camera useful to improve scintigraphic imaging interpretation? Nucl Med Commun. 2004; 25(7):705–10. [PubMed: 15208498]
33. Grant FD, et al. Skeletal PET with 18F-fluoride: applying new technology to an old tracer. J Nucl Med. 2008; 49(1):68–78. [PubMed: 18077529]
34. Thrall JH. Technetium-99m labeled agents for skeletal imaging. CRC Crit Rev Clin Radiol Nucl Med. 1976; 8(1):1–31. [PubMed: 789010]
35. Davis MA, Jones AL. Comparison of 99mTc-labeled phosphate and phosphonate agents for skeletal imaging. Semin Nucl Med. 1976; 6(1):19–31. [PubMed: 1108208]
36. Even-Sapir E. Imaging of malignant bone involvement by morphologic, scintigraphic, and hybrid modalities. J Nucl Med. 2005; 46(8):1356–67. [PubMed: 16085595]
37. Gralow JR, et al. NCCN Task Force Report: Bone Health in Cancer Care. J Natl Compr Canc Netw. 2009; 7(Suppl 3):S1–S32. quiz S33-S35. [PubMed: 19555589]
38. Bushnell DL, et al. Utility of SPECT imaging for determination of vertebral metastases in patients with known primary tumors. Skeletal Radiol. 1995; 24(1):13–6. [PubMed: 7709245]
39. Gnanasegaran G, et al. Multislice SPECT/CT in benign and malignant bone disease: when the ordinary turns into the extraordinary. Semin Nucl Med. 2009; 39(6):431–42. [PubMed: 19801222]
40. Zhao Z, et al. Single photon emission computed tomography/spiral computed tomography fusion imaging for the diagnosis of bone metastasis in patients with known cancer. Skeletal Radiol. 39(2): 147–53. [PubMed: 19669135]

NIH-PA Author Manuscript

NIH-PA Author Manuscript

NIH-PA Author Manuscript


41. Helyar V, et al. The added value of multislice SPECT/CT in patients with equivocal bony metastasis from carcinoma of the prostate. Eur J Nucl Med Mol Imaging. 2010; 37(4):706–13. [PubMed: 20016889]
42. Strobel K, et al. Characterization of focal bone lesions in the axial skeleton: performance of planar bone scintigraphy compared with SPECT and SPECT fused with CT. AJR Am J Roentgenol. 2007; 188(5):W467–74. [PubMed: 17449746]
43. Blau M, Nagler W, Bender MA. Fluorine-18: a new isotope for bone scanning. J Nucl Med. 1962; 3:332–4. [PubMed: 13869926]
44. Czernin J, Satyamurthy N, Schiepers C. Molecular mechanisms of bone 18F-NaF deposition. J Nucl Med. 51(12):1826–9. [PubMed: 21078790]
45. Cook GJ. PET and PET/CT imaging of skeletal metastases. Cancer Imaging. 10:1–8. [PubMed: 20663736]
46. Segall G, et al. SNM practice guideline for sodium 18F-fluoride PET/CT bone scans 1.0. J Nucl Med. 2010; 51(11):1813–20. [PubMed: 21051652]
47. Positron Emission Tomography (PET) (NaF-18) to Identify Bone Metastasis of Cancer. MLN Matters. 2011. Available from: https://www.cms.gov/MLNMattersArticles/downloads/MM6861.pdf
48. Yen RF, et al. The diagnostic and prognostic effectiveness of F-18 sodium fluoride PET-CT in detecting bone metastases for hepatocellular carcinoma patients. Nucl Med Commun. 2010; 31(7): 637–45. [PubMed: 20389259]
49. Kruger S, et al. Detection of bone metastases in patients with lung cancer: 99mTc-MDP planar bone scintigraphy, 18F-fluoride PET or 18F-FDG PET/CT. Eur J Nucl Med Mol Imaging. 2009; 36(11):1807–12. [PubMed: 19504092]
50. Fleming IN, et al. Opportunities for PET to deliver clinical benefit in cancer: breast cancer as a paradigm. Cancer Imaging. 10:144–52. [PubMed: 20605761]
51. Som P, et al. A fluorinated glucose analog, 2-fluoro-2-deoxy-D-glucose (F-18): nontoxic tracer for rapid tumor detection. J Nucl Med. 1980; 21(7):670–5. [PubMed: 7391842]
52. Pauwels EK, et al. Positron-emission tomography with [18F]fluorodeoxyglucose. Part I. Biochemical uptake mechanism and its implication for clinical studies. J Cancer Res Clin Oncol. 2000; 126(10):549–59. [PubMed: 11043392]
53. Basu S, Alavi A. Unparalleled contribution of 18F-FDG PET to medicine over 3 decades. J Nucl Med. 2008; 49(10):17N–21N. 37N.
54. Facey K, et al. Overview of the clinical effectiveness of positron emission tomography imaging in selected cancers. Health Technol Assess. 2007; 11(44):iii–iv. xi–267. [PubMed: 17999839]
55. Higashi K, et al. Fluorine-18-FDG PET imaging is negative in bronchioloalveolar lung carcinoma. J Nucl Med. 1998; 39(6):1016–20. [PubMed: 9627336]
56. Schoder H, Larson SM. Positron emission tomography for prostate, bladder, and renal cancer. Semin Nucl Med. 2004; 34(4):274–92. [PubMed: 15493005]
57. Carrasquillo JA, Chen CC. Molecular imaging of neuroendocrine tumors. Semin Oncol. 2010; 37(6):662–79. [PubMed: 21167384]
58. Pearse AG. The cytochemistry and ultrastructure of polypeptide hormone-producing cells of the APUD series and the embryologic, physiologic and pathologic implications of the concept. J Histochem Cytochem. 1969; 17(5):303–13. [PubMed: 4143745]
59. Pearse AG. The calcitonin secreting C cells and their relationship to the APUD cell series. J Endocrinol. 1969; 45(1):13–4. Suppl. [PubMed: 5347384]
60. Pearse AG. The APUD cell concept and its implications in pathology. Pathol Annu. 1974; 9(0):27–41. [PubMed: 4154097]
61. Pearse AG, Polak JM. Endocrine tumours of neural crest origin: neurolophomas, apudomas and the APUD concept. Med Biol. 1974; 52(1):3–18. [PubMed: 4157328]
62. De Visser M, et al. Stabilised 111In-labelled DTPA- and DOTA-conjugated neurotensin analogues for imaging and therapy of exocrine pancreatic cancer. European Journal of Nuclear Medicine and Molecular Imaging. 2003; 30(8):1134–1139. [PubMed: 12768332]

NIH-PA Author Manuscript

NIH-PA Author Manuscript

NIH-PA Author Manuscript


63. Hoyer D, et al. Classification and nomenclature of somatostatin receptors. Trends Pharmacol Sci. 1995; 16(3):86–8. [PubMed: 7792934]
64. Goldsmith SJ. Update on nuclear medicine imaging of neuroendocrine tumors. Future Oncol. 2009; 5(1):75–84. [PubMed: 19243300]
65. Haubner R, Decristoforo C. Radiolabelled RGD peptides and peptidomimetics for tumour targeting. Front Biosci. 2009; 14:872–86. [PubMed: 19273105]
66. Bombardieri E, et al. 111In-pentetreotide scintigraphy: procedure guidelines for tumour imaging. Eur J Nucl Med Mol Imaging. 2003; 30(12):BP140–7. [PubMed: 14989228]
67. Balon HR, et al. Procedure guideline for somatostatin receptor scintigraphy with (111)Inpentetreotide. J Nucl Med. 2001; 42(7):1134–8. [PubMed: 11438641]
68. Hofmann M, et al. Biokinetics and imaging with the somatostatin receptor PET radioligand (68)Ga-DOTATOC: preliminary data. Eur J Nucl Med. 2001; 28(12):1751–7. [PubMed: 11734911]
69. Kroiss A, et al. Functional imaging in phaeochromocytoma and neuroblastoma with 68Ga-DOTA-Tyr 3-octreotide positron emission tomography and 123I-metaiodobenzylguanidine. Eur J Nucl Med Mol Imaging. 2011; 38(5):865–73. [PubMed: 21279352]
70. Gabriel M, et al. 68Ga-DOTA-Tyr3-octreotide PET for assessing response to somatostatin-receptor-mediated radionuclide therapy. J Nucl Med. 2009; 50(9):1427–34. [PubMed: 19690033]
71. Shields AF, et al. Imaging proliferation in vivo with [F-18]FLT and positron emission tomography. Nat Med. 1998; 4(11):1334–6. [PubMed: 9809561]
72. Vallabhajosula S. (18)F-labeled positron emission tomographic radiopharmaceuticals in oncology: an overview of radiochemistry and mechanisms of tumor localization. Semin Nucl Med. 2007; 37(6):400–19. [PubMed: 17920348]
73. Salskov A, et al. FLT: measuring tumor cell proliferation in vivo with positron emission tomography and 3'-deoxy-3'-[18F]fluorothymidine. Semin Nucl Med. 2007; 37(6):429–39. [PubMed: 17920350]
74. Shields AF, et al. Carbon-11-thymidine and FDG to measure therapy response. J Nucl Med. 1998; 39(10):1757–62. [PubMed: 9776283]
75. Wells P, et al. Assessment of proliferation in vivo using 2-[(11)C]thymidine positron emission tomography in advanced intra-abdominal malignancies. Cancer Res. 2002; 62(20):5698–702. [PubMed: 12384527]
76. Eary JF, et al. 2-[C-11]thymidine imaging of malignant brain tumors. Cancer Res. 1999; 59(3): 615–21. [PubMed: 9973209]
77. Del Vecchio S, et al. PET/CT in cancer research: from preclinical to clinical applications. Contrast Media Mol Imaging. 2010; 5(4):190–200. [PubMed: 20812287]
78. Barwick T, et al. Molecular PET and PET/CT imaging of tumour cell proliferation using F-18 fluoro-L-thymidine: a comprehensive evaluation. Nucl Med Commun. 2009; 30(12):908–17. [PubMed: 19794320]
79. Folkman J. Tumor angiogenesis: therapeutic implications. N Engl J Med. 1971; 285(21):1182–6. [PubMed: 4938153]
80. Faivre S, et al. Molecular basis for sunitinib efficacy and future clinical development. Nat Rev Drug Discov. 2007; 6(9):734–45. [PubMed: 17690708]
81. Cai W, Niu G, Chen X. Imaging of integrins as biomarkers for tumor angiogenesis. Curr Pharm Des. 2008; 14(28):2943–73. [PubMed: 18991712]
82. Cai W, Chen X. Multimodality molecular imaging of tumor angiogenesis. J Nucl Med. 2008; 49(Suppl 2):113S–28S. [PubMed: 18523069]
83. Cai W, Gambhir SS, Chen X. Chapter 7. Molecular imaging of tumor vasculature. Methods Enzymol. 2008; 445:141–76. [PubMed: 19022059]
84. Hynes RO, et al. The diverse roles of integrins and their ligands in angiogenesis. Cold Spring Harb Symp Quant Biol. 2002; 67:143–53. [PubMed: 12858535]
85. Hynes RO. Integrins: bidirectional, allosteric signaling machines. Cell. 2002; 110(6):673–87. [PubMed: 12297042]

NIH-PA Author Manuscript

NIH-PA Author Manuscript

NIH-PA Author Manuscript


86. Hynes RO. A reevaluation of integrins as regulators of angiogenesis. Nat Med. 2002; 8(9):918–21. [PubMed: 12205444]
87. Hood JD, Cheresh DA. Role of integrins in cell invasion and migration. Nat Rev Cancer. 2002; 2(2):91–100. [PubMed: 12635172]
88. Hood JD, et al. Tumor regression by targeted gene delivery to the neovasculature. Science. 2002; 296(5577):2404–7. [PubMed: 12089446]
89. Haubner R, et al. Glycosylated RGD-containing peptides: tracer for tumor targeting and angiogenesis imaging with improved biokinetics. J Nucl Med. 2001; 42(2):326–36. [PubMed: 11216533]
90. Haubner R, et al. Noninvasive imaging of alpha(v)beta3 integrin expression using 18F-labeled RGD-containing glycopeptide and positron emission tomography. Cancer Res. 2001; 61(5):1781–5. [PubMed: 11280722]
91. Beer AJ, et al. PET-based human dosimetry of 18F-galacto-RGD, a new radiotracer for imaging alpha v beta3 expression. J Nucl Med. 2006; 47(5):763–9. [PubMed: 16644745]
92. Beer AJ, Schwaiger M. Imaging of integrin alphavbeta3 expression. Cancer Metastasis Rev. 2008; 27(4):631–44. [PubMed: 18523730]
93. Beer AJ, et al. Comparison of integrin alphaVbeta3 expression and glucose metabolism in primary and metastatic lesions in cancer patients: a PET study using 18F-galacto-RGD and 18FFDG. J Nucl Med. 2008; 49(1):22–9. [PubMed: 18077538]
94. Haubner R. Alphavbeta3-integrin imaging: a new approach to characterise angiogenesis? Eur J Nucl Med Mol Imaging. 2006; 33(Suppl 1):54–63. [PubMed: 16791598]
95. Delso G, Ziegler S. PET/MRI system design. European journal of nuclear medicine and molecular imaging. 2009; 36(Suppl 1):S86–92. [PubMed: 19104809]
96. Zaidi H, et al. Design and performance evaluation of a whole-body Ingenuity TF PET-MRI system. Physics in medicine and biology. 2011; 56(10):3091–106. [PubMed: 21508443]
97. von Schulthess GK, Schlemmer HP. A look ahead: PET/MR versus PET/CT. European journal of nuclear medicine and molecular imaging. 2009; 36(Suppl 1):S3–9. [PubMed: 19104804]
98. Antoch G, Bockisch A. Combined PET/MRI: a new dimension in whole-body oncology imaging? European journal of nuclear medicine and molecular imaging. 2009; 36(Suppl 1):S113–20. [PubMed: 19104802]

NIH-PA Author Manuscript
NIH-PA Author Manuscript
NIH-PA Author Manuscript



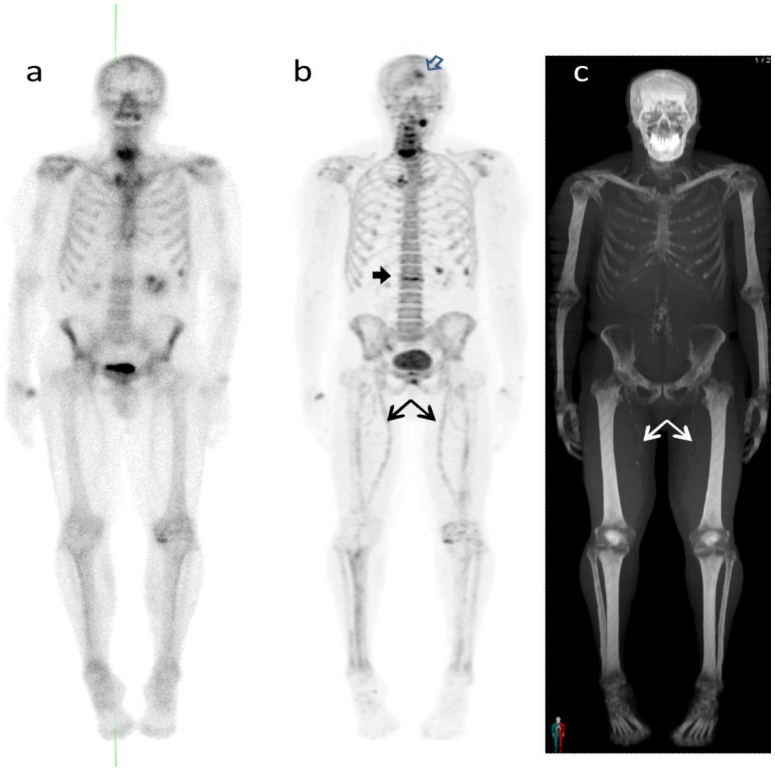


**Figure 1.**

77 year old male with prostate cancer: **a.** Anterior planar gamma camera image acquired 3-hours post injection of 12mCi $^{99m}$Tc-MDP; **b.** Anterior coronal Maximum pixel Intensity Projection (MIP) PET emission scan acquired 2-hours post injection of 5.1 mCi Na$^{18}$F; **c.** Anterior MIP of the transmission CT. Noted improved spatial resolution on the PET image, with better visualization of the skull lesion (open arrow) and L1/2 degenerative disc disease (solid arrow). Even the calcification of the femoral arteries (arrows) is visualized on the PET image. Careful correlation with the transmission CT is needed to determine etiology of focal uptake.

NIH-PA Author Manuscript
NIH-PA Author Manuscript
NIH-PA Author Manuscript



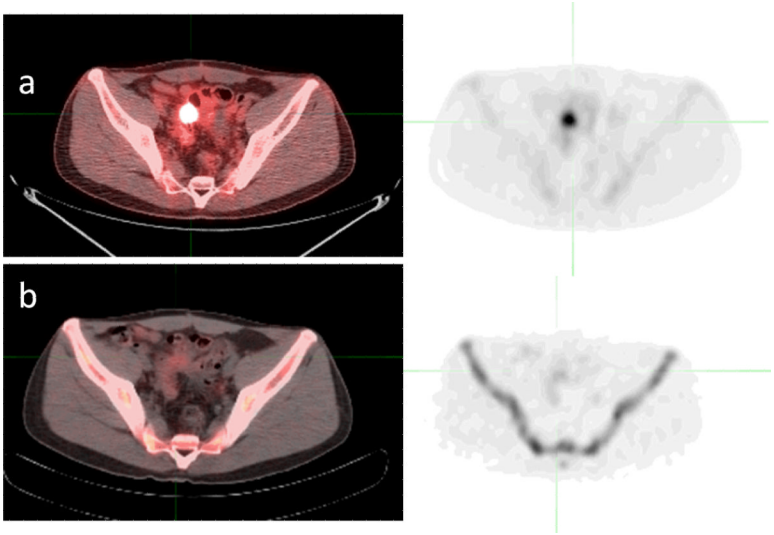


**FIGURE 2.**

37 yo, male with history of Large B-cell lymphoma in small bowel extending to posterior bladder. Residual pelvic residual mass was seen after chemotherapy which shows high $^{18}$F-FDG uptake (a) SUV 10.4, and no significant $^{18}$FLT uptake (b) SUV 2.2. Biopsy revealed fibrosis/chronic inflammatory changes in an enterovesicular fistula.

NIH-PA Author Manuscript

NIH-PA Author Manuscript

NIH-PA Author Manuscript

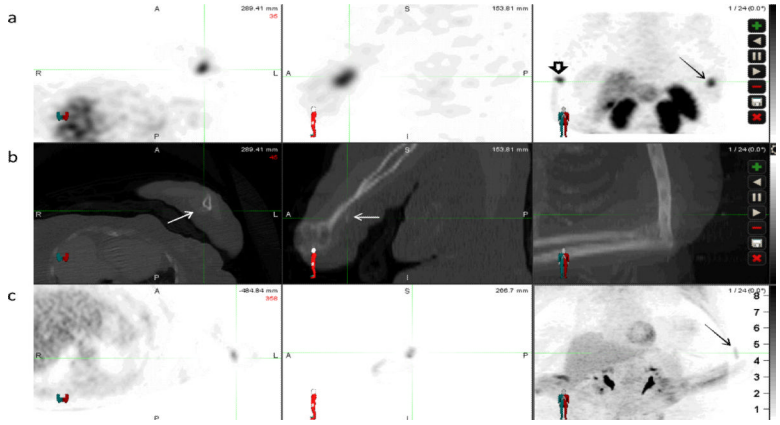


**Figure 3.**

66 year old female with tumor induced osteomalacia. Row (a) displays SPECT images (axial, sagittal, and Maximum pixel Intensity Projection (MIP)) obtained 4-hours after the injection of 6.5mCi $^{111}$In- DPTA-pentreotide; row (b) displays the transmission CT from that study; row (c) displays PET scan acquired 1-hour post injection of 14.4mCi of $^{18}$F-FDG. The intense focal uptake in the distal left arm (cross hairsc and solid arrow) on the $^{111}$In- DPTA-pentreotide SPECT images, which corresponds to faint soft tissue calcifications on the transmission CT, shows only mild uptake on the $^{18}$F-FDG PET images. (Open arrow indicates injection site)

NIH-PA Author Manuscript
NIH-PA Author Manuscript
NIH-PA Author Manuscript



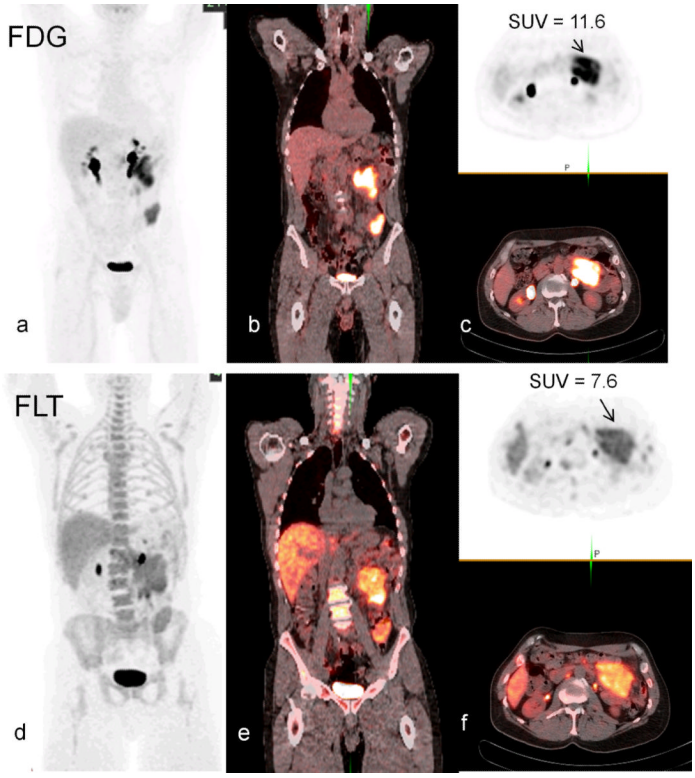


**Figure 4.**
Comparison of PET/CT scans of the same patient with abdominal lymphomas using the tracers $^{18}$F-FDG (a,b,c) and $^{18}$F-FLT (d,e,f) (MIP (a,d), coronal fused (b,e) and axial/axial fused views (c,f))

NIH-PA Author Manuscript

NIH-PA Author Manuscript

NIH-PA Author Manuscript

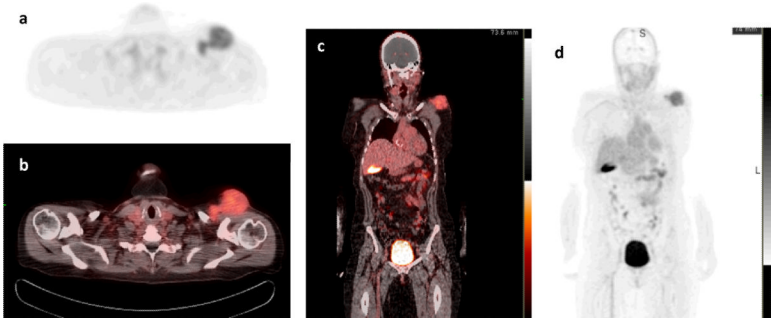


**Figure 5.**

$^{18}$F-Fluciclatide PET (a,d) and PET/CT (b,c) scan of a patient with metastatic melanoma using (axial (a,b) and coronal (c,d)). Note the specific localization of tracer uptake to the left shoulder. The remaining tracer distribution is physiologic.

NIH-PA Author Manuscript

NIH-PA Author Manuscript

NIH-PA Author Manuscript

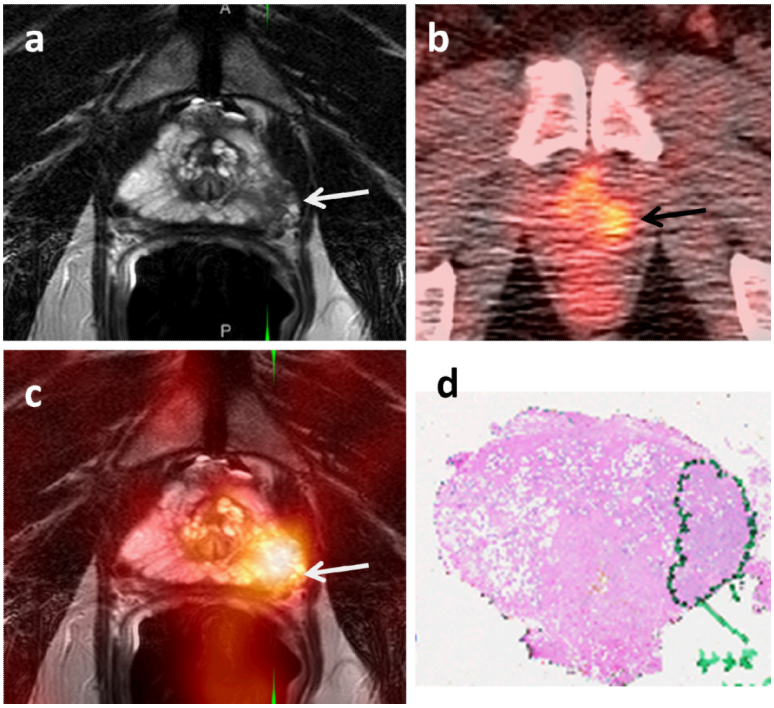


**Figure 6.**

55-year-old male with prostate cancer. Axial T2-weighted MRI (a) demonstrates a low signal intensity focus in the left apical gland peripheral zone (white arrow), which shows $^{11}$C-Acetate uptake in the axial PET/CT image (black arrow) (b). Software based fused $^{11}$C-Acetate PET/MR image (c) better localizes the tumor focus (white arrow). Corresponding pathology slide shows a Gleason 3+4 tumor lesion in the left apical peripheral zone (inked in green) (d).

NIH-PA Author Manuscript

NIH-PA Author Manuscript

NIH-PA Author Manuscript

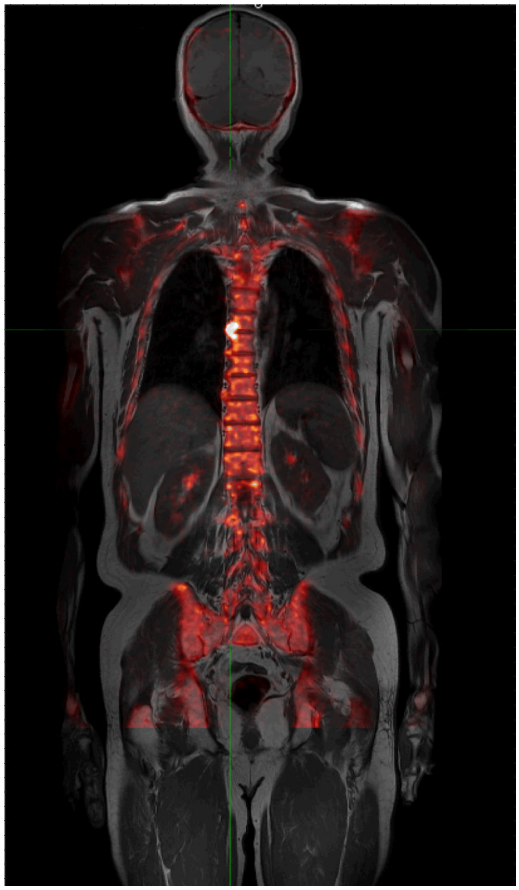

**Figure 7.**
Whole body PET MR performed on the Siemens whole body mMR MR/PET scanner ~4 hours following administration of 3.3mCi of $^{18}$F-NaF in a 63 year old patient with prostate cancer (Gleason 3+4). This study shows increased bony turnover in the mid-T-spine (SUV =29.7) in a location consistent with degenerative change. No bony metastatic disease was detected. Whole body coronal STIR MR sequence is shown.

NIH-PA Author Manuscript

NIH-PA Author Manuscript

NIH-PA Author Manuscript

## Table 1

| Type | Clinically Available | Research Use Only |
|---|---|---|
| General Tumor Imaging | $^{18}$F-FDG | $^{18}$F-FLT |
| Somatostatin receptor Imaging | $^{111}$In-DTPA-pentreotide<br>$^{131}$I-metaiodobenzylguanidine (MIBG)<br>$^{123}$I-MIBG (iobenguane/Adreview) | $^{99m}$Tc-EDDA/HYNIC-TOC<br>$^{68}$GaDOTA TOC |
| Bone imaging | $^{99m}$Tc-MDP<br>$^{18}$F-NaF | |
| Angiogenesis | | $^{18}$F-galacto-RGD<br>$^{18}$F-Fluciclatide |